4186 *Inorg. Chem.* **2010**, *49*, 4186–4193
DOI: 10.1021/ic902417m

Inorganic Chemistry
Article

Photophysical Properties of Ruthenium(II) Polypyridyl-Gold(I) Ethynyl Dyads and Triads Containing Mono- or Diethynylphenanthroline Incorporated into Gold(I) Triphenylphosphine Organometallics

Michito Shiotsuka,*,† Yasushi Tsuji,† Kazutoshi Keyaki,‡ and Koichi Nozaki‡

†*Graduate School of Engineering, Nagoya Institute of Technology, Showa-ku, Nagoya, Aichi 466-8555, Japan, and* ‡*Department of Chemistry, Graduate School of Science and Engineering, University of Toyama, 3190, Gofuku, Toyama-shi, Toyama 930-8555, Japan*

Received December 5, 2009

A new ruthenium(II)−gold(I) dyad, $[Ru(bpy)_2\{5\text{-}\{(PPh_3)-Au-C\equiv C\}\text{-phen}\}](PF_6)_2$ (**2**), with a different substituted site compared to $[Ru(bpy)_2\{3\text{-}\{(PPh_3)-Au-C\equiv C\}\text{-phen}\}](PF_6)_2$ (**1**), and a triad, $[Ru(bpy)_2\{3,6\text{-bis-}\{(PPh_3)-Au-C\equiv C\}\text{-phen}\}](PF_6)_2$ (**3**), with an unsymmetric diethynylphenanthroline relative to $[Ru(bpy)_2\{3,8\text{-bis}\{(PPh_3)-Au-C\equiv C\}\text{-phen}\}](PF_6)_2$ (**4**) have been prepared. These four ruthenium(II)−gold(I) compounds showed typical metal-to-ligand charge-transfer (MLCT) absorption bands in the 400−550 nm region and a lowest energy $\pi-\pi^*$ absorption involved with the gold(I) perturbation in the 300−400 nm region. Broad emission bands assignable to the triplet MLCT transition were definitely observed in all compounds, indicating that the hybrid architecture constructed with Ru(II)-polypyridyl and Au(I)-ethynyl units converts the blue-green gold(I) perturbed $\pi-\pi^*$ phosphorescence into an orange MLCT-based emission. The transient absorption difference spectra of four compounds showed the difference in the electron transfer process between **2** and other compounds **1**, **3**, and **4** under the excited state. Ru(II)−Au(I) compounds except for **2** receive the supposed charge injection from a ruthenium center to an extended π-conjugated ethynyl-substituted phenanthroline, which contains one or two gold(I) organometallic unit(s), while **2** undergoes the electron transfer process from the ruthenium center not to the 5-ethynylphenanthroline but to one of the bipyridyl ligands under the excited state. This hypothesis is supported by the deflection of the spots of **2** and $[Ru(bpy)_3](PF_6)_2$ from a linear correlation line in a plot of $E(0-0)$ versus $\Delta E_{1/2}$, which was based on the electrochemical and emission data of Ru(II)−Au(I) compounds and mononuclear ruthenium(II) polypyridyl complexes.

Introduction

Over the past few decades, there has been increasing interest in the study of photoactive multicomponent molecular systems, including photoactive metal complex subunits, because of their potential applications in the field of optoelectronic devices and solar energy conversion.[1,2] Extensive photophysical studies of the multicomponent system, including ruthenium(II) polypyridyl complexes, have been carried out, and the energy and/or electron transfer processes among several subunits in the multicomponent system under the photoexcited state have been revealed.[1−4] The study of a photoactive molecular system with ruthenium(II) polypyridyl complexes containing ethynyl-substituted bipyridyl and terpyridyl ligands has been particularly reported in the past two decades.[5−13] In this regard, we have previously reported the photophysical and electrochemical properties of ruthenium(II) polypyridyl complexes containing 3-ethynylphenanthroline

*To whom correspondence should be addressed. E-mail: michito@nitech.ac.jp.

(1) Balzani, V.; Credi, A.; Venturi, M. *Molecular Devices and Machines*; Wiley-VCH: Germany, 2004 (and references therein).
(2) Balzani, V.; Bergamini, G.; Campagna, S.; Puntoriero, F. *Top. Curr. Chem.* **2007**, *280*, 1.
(3) Julis, A.; Balzani, V.; Baligelletti, F.; Campagna, S.; Belser, P.; Zelewsky, A. V. *Coord. Chem. Rev.* **1998**, *84*, 85.
(4) Campagna, S.; Puntoriero, F.; Nastasi, F.; Bergamini, G.; Balzani, V. *Top. Curr. Chem.* **2007**, *280*, 117.
(5) Harriman, A.; Ziessel, R. *Coord. Chem. Rev.* **1998**, *171*, 331.
(6) Ziessel, R.; Hissler, M.; El-ghayoury, A.; Harriman, A. *Coord. Chem. Rev.* **1998**, *178*, 1251.
(7) Kozlov, D. V.; Tyson, D. S.; Goze, C.; Ziessel, R.; Castellano, F. N. *Inorg. Chem.* **2004**, *43*, 6083.
(8) Barbieri, A.; Ventura, B.; Flamigni, L.; Barigelletti, F.; Fuhrmann, G.; Bäuerle, P.; Goeb, S.; Ziessel, R. *Inorg. Chem.* **2005**, *44*, 8033.
(9) Galletta, M.; Campagna, S.; Quesada, M.; Ulrich, G.; Ziessel, R. *Chem. Commun.* **2005**, 4222.
(10) Harriman, A.; Mayeux, A.; Stroh, C.; Ziessel, R. *Dalton Trans.* **2005**, 2925.
(11) Benniston, A. C.; Hariman, A.; Li, P.; Sams, C. A. *J. Am. Chem. Soc.* **2005**, *127*, 2553.
(12) Leventis, N.; Rawashdeh, A.-M. M.; Elder, I. A.; Yang, J.; Dass, A.; Sotiriou-Leventis, C. *Chem. Mater.* **2004**, *16*, 1493.
(13) Fan., Y.; Zhang, L.-Y. ; Dai, F.-R.; Shi, L.-X. ; Chen, Z.-N. *Inorg. Chem.* **2008**, *47*, 2811.

 Published on Web 04/05/2010 © 2010 American Chemical Society

and 3,8-diethynylphenanthroline linked by gold(I) triphenylphosphine organometallics, which are $[Ru(bpy)_2\{3\text{-}\{(PPh_3)-Au-C\equiv C\}\text{-phen}\}](PF_6)_2$ (**1**) and $[Ru(bpy)_2\{3,8\text{-bis}\{(PPh_3)-Au-C\equiv C\}\text{-phen}\}](PF_6)_2$ (**4**) (Chart 1), and this multicomponent system indicates the supposed charge injection from a ruthenium center to an extended π-conjugated ethynylphenanthroline ligand containing gold(I) triphenylphosphine organometallic unit(s) under the photoexcited state.[14] Furthermore, a study of dinuclear ruthenium(II) polypyridyl complexes containing the bridging ligand of two bipyridine units linked at the 4-, 5-, and 6-substitutions with an acetylide unit by Ziessel et al.[15] and a photophysical study of ruthenium(II) polypyridyl complexes containing 4,4′- and 5,5′-phenylethynyl-substituted bipyridine by Schanze et al.[16] suggest a distinguishing difference in the emission energy from the metal-to-ligand charge-transfer (MLCT) transition among these ruthenium(II) complexes including an ethynyl-substituted ligand with a different substituted site. Recently, an interesting photophysical property of mononuclear ruthenium(II) complexes with phenylethynylphenanthrolines with a different substitution, $[Ru(bpy)_2\{X\text{-phenylethynyl-1,10-phen}\}](PF_6)_2$ (X = 3, 4, and 5), have been reported by Tor et al.[17] The 3- and 5-substituted compounds have shown a usual triplet MLCT emission, while the 4-substituted compound has displayed a dual emission assigned to two transitions of different triplet MLCT states. However, a distinct difference in the photophysical properties between 3- and 5-substituted compounds was not reported.

In contrast, current research regarding gold(I) alkynyl complexes has gained significance with respect to their potential applications in nanomaterials due to their particularly interesting properties as luminescent chemosensors.[18] Synthesis and photophysical study of gold(I) ethynyl-substituted polyimine complexes containing bipyridine or phenanthroline or terpyridine have been reported by Vicente et al.[19] and our group,[20,21] and the phosphorescence and dual emissions of gold(I) ethynyl-substituted polyimine complexes have been revealed. We have recently reported a distinguishing difference in emission spectra between two gold(I) complexes with different substituted sites, $3\text{-}\{(PPh_3)-Au-C\equiv C\}$-phen and $5\text{-}\{(PPh_3)-Au-C\equiv C\}$-phen.[20] Furthermore, in photophysical research of the dinuclear gold(I) complexes 3,6-bis$\{(PPh_3)-Au-C\equiv C\}_2$-phen and 3,8-bis$\{(PPh_3)-Au-C\equiv C\}_2$-phen, the higher energy $\pi-\pi^*$ absorption and lower energy phosphorescence in the unsymmetrical 3,6-substituted complex than in the symmetrical 3,8-substituted complex have been revealed.[20]

We report herein the synthesis of a new ruthenium(II)−gold(I) dyad, $[Ru(bpy)_2\{5\text{-}\{(PPh_3)-Au-C\equiv C\}\text{-phen}\}](PF_6)_2$ (**2**), with a different substituted site compared with the dyad **1** and triad, $[Ru(bpy)_2\{3,6\text{-bis}\{(PPh_3)-Au-C\equiv C\}\text{-phen}\}](PF_6)_2$ (**3**), with an unsymmetric diethynylphenanthroline relative to the triad **4**, and the photophysical and electrochemical properties of these ruthenium(II)−gold(I) compounds (Chart 1). This study has focused on the photophysical effects of introducing a different substitution site for the gold(I) ethynyl unit, $-C\equiv C-Au-PPh_3$, to the phenanthroline skeleton in these ruthenium(II)−gold(I) compounds. Electrochemical measurements were performed to obtain the potential difference between the oxidation and the first reduction potentials in Ru(II)−Au(I) compounds and mononuclear ruthenium(II) polypyridyl complexes because most of the ruthenium(II) complexes $[Ru(bpy)_2(L\text{-}L)](PF_6)_2$ (L-L = diimine and its derivatives) have a good linear correlation between the potential difference based on the electrochemical data and the triplet MLCT transition energy estimated with the emission spectral data. The dynamics of the triplet MLCT state are probed using the transient absorption difference and time-resolved emission spectroscopy. These results for the Ru(II)−Au(I) compounds show a unique difference in the electron transfer process between **2** and three other Ru(II)−Au(I) compounds **1**, **3**, and **4** under the triplet MLCT state.

Chart 1. Structures of Ru(II)−Au(I) and Precursor Ruthenium Complexes

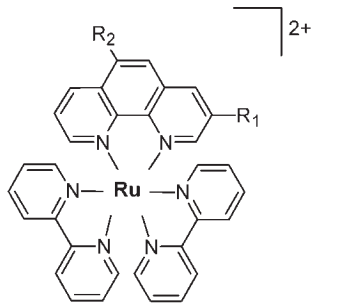

1: R_1 = ≡—Au-PPh_3, R_2 = H
2: R_1 = H, R_2 = ≡—Au-PPh_3
3: R_1 = ≡—Au-PPh_3, R_2 = ≡—Au-PPh_3
5: R_1 = ≡—H, R_2 = H
6: R_1 = H, R_2 = ≡—H
7: R_1 = ≡—H, R_2 = ≡—H

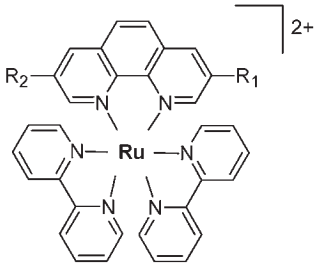

4: R_1 = ≡—Au-PPh_3, R_2 = ≡—Au-PPh_3
8: R_1 = ≡—H, R_2 = ≡—H

Experimental Section

Structural formulas and abbreviations for the compounds studied are given in Chart 1.

Materials and Measurements. The starting materials were purchased from Aldrich or Nacalai and used without further

(14) Shiotsuka, M.; Yamamoto, Y.; Okuno, S.; Kitou, M.; Nozaki, K.; Onaka, S. *Chem. Commun.* **2002**, 590.
(15) Grosshenny, V.; Harriman, A.; Romero, F. M.; Ziessel, R. *J. Phys. Chem.* **1996**, *100*, 17472.
(16) Wang, Y.; Liu, S.; Pinto, M. R.; Dattelbaum, D. M.; Schoonover, J. R.; Schanze, K. S. *J. Phys. Chem. A* **2001**, *105*, 11118.
(17) Glazer, E. C.; Magde, D.; Tor, Y. *J. Am. Chem. Soc.* **2007**, *129*, 8544.
(18) (a) Tang, H.-S.; Zhu, N.; Yam, V. W.-W. *Organometallics* **2007**, *26*, 22. (b) Lu, X.-X. ; Li, C.-K.; Cheng, E. C.-C.; Zhu, N.; Yam, V. W.-W. *Inorg. Chem.* **2004**, *43*, 2225.
(19) Vicente, J.; Gil-Rubio, J.; Barquero, N.; Jones, P. G.; Bautista, D. *Organometallics* **2008**, *27*, 646.
(20) Shiotsuka, M.; Nishiko, N.; Tsuji, Y.; Kitamura, N.; Onaka, S.; Sako, K. *Transition Met. Chem.* **2010**, *35*, 129.
(21) Yamamoto, Y.; Shiotsuka, M.; Okuno, S.; Onaka, S. *Chem. Lett.* **2004**, *33*, 210.

purification. Solvents were freshly distilled according to standard procedures. All reactions were carried out under an argon or a nitrogen atmosphere. Precursor ruthenium(II) complexes **5**, **6**, **7**, and **8** (See Chart 1) were synthesized by the similar method of Tor et al.[22] The syntheses of $[Ru(bpy)_2L1](PF_6)_2$ (L1 = 3-*p*-tolylethynyl-phenanthroline) and $[Ru(bpy)_2L2](PF_6)_2$ (L2 = 3,8-bis-*p*-tolylethynyl-phenanthroline) have been reported by our previous paper.[23] Characterization of the Ru(II)−Au(I) compounds has been done by IR, ^{1}H NMR, UV−vis, emission, electrospray ionization mass (ESI-MS) spectroscopy, and elemental analysis. Elemental analysis was performed for C, H, and N elements on a Perkin-Elmer 2400II CHNS/O full-automatic analyzer. The ESI-MS spectra were acquired using an LCT mass spectrometer equipped with an ion spray interface (Micromass Limited, Manchester, U.K.). Samples were introduced using a single syringe pump (KD Scientific Inc.) fitted with Hamilton syringes (Hamilton Co., Reno, NE). The samples employed for spectral measurements were prepared in acetonitrile (HPLC grade). FT-IR spectra were obtained on a JASCO FT/IR 460 spectrometer using the KBr-pellet method. The ^{1}H NMR spectra were recorded with a Bruker AVANCE NMR spectrometer (600 MHz) at room temperature, and the chemical shifts were referenced to tetramethylsilane ($SiMe_4$). UV−vis spectra were recorded on a SHIMADZU U-1800 spectrophotometer in CH_3CN (spectroscopic grade) at room temperature.

Electrochemical measurement was performed by using a BAS CV-50W Voltammetric Analyzer. Measurement was made in N_2-purged acetonitrile containing 0.1 M $[N(n\text{-}C_4H_9)_4](PF_6)$ in a three-compartment cell. A platinum coil counter, a platinum wire working electrode, and $Ag/AgNO_3$ reference electrode (+0.37 V vs SCE; calibrated with $Fc^{+/0}$) were used. The $E_{1/2}$ values were calculated as the average of the anodic and cathodic peak potentials, $(E_{pa} + E_{pc})/2$, from cyclic voltammogram data.

The corrected emission spectra were measured with a HAMAMATSU C7473 photonic multichannel analyzer, and excitation spectra were recorded on a HITACHI F-2500 fluorescence spectrophotometer. Emission spectra for quantum yield measurement at room temperature were measured in degassed acetonitrile by argon bubbling (over 20 min) upon excitation at 425 nm. Emission spectra at 77 K were measured using a liquid nitrogen in a quarts Dewar vessel upon excitation at 425 nm, and sample solutions (ethanol) in a 5 mm quarts sealed tube were deaerated by freeze−pump−thaw (4 times). The corrected emission spectral data were converted the emission intensity in terms of units of energy emitted per energy interval for spectral analysis. The 0−0 band energy, $E(0-0)$, and the emission spectral fitting parameters were calculated with the method of Franck−Condon analysis developed by Meyer's group.[24,25] These calculated parameters and details of the calculation are described in the Supporting Information.

Nanosecond time-resolved transient absorption (TA) spectra were obtained by using the third harmonic of a Q-switched Nd^{3+}:YAG laser (Continuum Surelite I-10, λ = 355 nm). Sample solutions in a 1 cm quartz cell were deaerated by bubbling with argon for 10 min. White light from a Xe-arc lamp was used for acquisition of absorption spectra. For the determination of emission lifetimes, samples were irradiated using the third harmonic pulses of the Nd^{3+}:YAG laser. The emission from the samples was passed through a grating monochromator (H-10, Jobin Yvon) to eliminate scattering light and focused into a Si avalanche photodiode (Si-APD, S5139, Hamamatsu). The photocurrent from the Si-APD was amplified through wide-band amplifier (DC-500 MHz, CLC110) and accumulated on a digitizing oscilloscope (HP 54520 Hewlett-Packard) to get the decay profile of the emission intensity, which was fit to a single-exponential function with convolution of the instrumental response function of the measuring system. The time resolution of the system is 2 ns.

Synthesis of $[Ru(bpy)_2\{3\text{-}\{(PPh_3)-Au-C\equiv C\}\text{-}phen\}](PF_6)_2$ (1). Gold(I) complex $Au(PPh_3)Cl$ (50 mg, 0.10 mmol) and diisopropylamine (0.5 mL) were added successively to the CH_2Cl_2 (50 mL) solution of **5** (91 mg, 0.10 mmol) under N_2. After the mixture was stirred at 30 °C for 20 h, the solvent and excess diisopropylamine were removed under reduced pressure. The residue was redissolved in CH_3CN-H_2O (8:2) (50 mL), and acetonitrile was slowly evaporated until an orange-red compound was precipitated (100 mg, 73%). Anal. Calcd for $C_{52}H_{38}N_6P_3F_{12}Au_1Ru_1\cdot H_2O_1$: C, 45.13; H, 2.91; N, 6.07. Found: C, 44.80; H, 2.76; N, 5.94%. Positive ESI-MS: ion at m/z 538.5 (M^{2+}, 100%). FT-IR (KBr, cm^{-1}) ν(C≡C): 2112. UV/vis (CH_3CN): λ_{abs} nm ($\varepsilon \times 10^{-4}$) 452 (1.1), 423 (1.0), 342 (2.1), 286 (6.4). ^{1}H NMR (CD_3CN, 600 MHz, ppm): δ = 8.562 (dd, J = 8.2 and 1.0 Hz, 1H, phen-H7), 8.527 (m, 1H, bpy-H6α), 8.518 (m, 1H, bpy-H6β), 8.491 (m, 1H, bpy-H6′α), 8.488 (d, J = 1.7 Hz, 1H, phen-H4), 8.478 (m, 1H, bpy-H6′β), 8.191 (d, J = 8.9 Hz, 1H, phen-H5), 8.115 (d, J = 8.9 Hz, 1H, phen-H6), 8.087 (m, 1H, bpy-H5α), 8.078 (m, 1H, bpy-H5β), 8.035 (dd, J = 5.2 and 1.0 Hz, 1H, phen-H9), 8.006 (m, 1H, bpy-H5′α), 7.980 (m, 1H, bpy-H5′β), 7.950 (d, J = 1.7 Hz, 1H, phen-H2), 7.856 (m, 1H, bpy-H3α), 7.797 (m, 1H, bpy-H3β), 7.689 (dd, J = 8.2 and 5.0 Hz, 1H, phen-H8), 7.620 (m, 1H, bpy-H3′α), 7.525 (m, 1H, bpy-H3′β), 7.440 (m, 1H, bpy-H4α), 7.436 (m, 1H, bpy-H4β), 7.239 (m, 1H, bpy-H4′α), 7.228 (m, 1H, bpy-H4′β), 7.66−7.51 (m, 15H, phenyl-H).

Synthesis of $[Ru(bpy)_2\{5\text{-}\{(PPh_3)-Au-C\equiv C\}\text{-}phen\}](PF_6)_2$ (2). A 91 mg portion of **6** (0.10 mmol) and NaOMe (32 mg, 0.60 mmol) were dissolved in a solution mixture of CH_3OH/CH_2Cl_2 (50 mL/10 mL) under Ar. The solution was added $Au(PPh_3)Cl$ (49.5 mg, 0.10 mmol), and the mixture was stirred at 30 °C under Ar. After 3 h, the solution was concentrated until about 10 mL of the volume by an evaporator and added to the water (20 mL) containing NH_4PF_6 (163 mg, 1.0 mmol). The orange precipitate was collected by filtration with a suction filter and washed with water (30 mL) and ether (30 mL). An orange-red powder was dried at 40 °C under vacuum for 3 h (125 mg, 92%). Anal. Calcd for $C_{52}H_{38}N_6P_3F_{12}Au_1Ru_1\cdot H_2O_1$: C, 45.13; H, 2.91; N, 6.07. Found: C, 45.06; H, 2.80; N, 5.74%. Positive ESI-MS: ion at m/z 538.5 (M^{2+}, 100%). FT-IR (KBr, cm^{-1}) ν(C≡C): 2093. UV/vis (CH_3CN): λ_{abs} nm ($\varepsilon \times 10^{-4}$) 452 (1.6), 428 (1.4), 331(2.1), 280 (7.8). ^{1}H NMR (CD_3CN, 600 MHz, ppm): δ = 9.038 (d, J = 8.3 Hz, 1H, phen-H4), 8.520 (m, 2H, bpy-H6), 8.487 (d, J = 8.3 Hz, 1H, phen-H7), 8.475 (m, 2H, bpy-H6′), 8.227 (s, 1H, phen-H6), 8.094 (m, 2H, bpy-H5), 8.076 (d, J = 5.2 Hz, 1H, phen-H9), 7.997 (d, J = 5.2 Hz, 1H, phen-H2), 7.984 (m, 2H, bpy-H5′), 7.832 (m, 2H, bpy-H3), 7.763 (dd, J = 8.3 and 5.2 Hz, 1H, phen-H8), 7.671 (dd, J = 8.3 and 5.2 Hz, 1H, phen-H8), 7.436 (m, 2H, bpy-H4), 7.222 (m, 2H, bpy-H4′), 7.62-7.50 (m, 15H, phenyl-H and phen-H3).

Synthesis of $[Ru(bpy)_2\{3,6\text{-}bis\{(PPh_3)-Au-C\equiv C\}\text{-}phen\}](PF_6)_2$ (3). Complex **7** (100 mg, 0.107 mmol) and diisopropylamine (1.3 mL) were dissolved in a mixed solvent of CH_3OH/CH_2Cl_2 (65 mL/25 mL) under Ar. The solution was added successively $Au(PPh_3)Cl$ (106 mg, 0.214 mmol), and the mixture was stirred at 30 °C under Ar. After 20 h, an orange-red precipitate appeared in the solution. The precipitate was collected by filtration under low-pressure and washed with a small amount of EtOH. An orange-red powder was dried at 30 °C under vacuum for 5 h (158 mg, 80%). Anal. Calcd for $C_{72}H_{52}N_6P_4F_{12}Au_2Ru_1$: C, 46.46; H, 3.06; N, 4.69. Found C, 46.75; H, 2.84; N, 4.55%. Positive ESI-MS: ion at m/z 778.8

(22) Connors, P. J., Jr.; Tzalis, D.; Dunnick, A. L.; Tor, Y. *Inorg. Chem.* **1998**, *37*, 1121.
(23) Shiotsuka, M.; Inui, Y.; Sekioka, Y.; Yamamoto, Y.; Onaka, S. *J. Organomet. Chem.* **2007**, *692*, 2441.
(24) Kober, E. M.; Casper, J. V.; Lumpkin, R. S.; Meyer, T. J. *J. Phys. Chem.* **1986**, *90*, 3722.
(25) Allen, G. H.; White, R. P.; Rillema, D. P.; Meyer, T. J. *J. Am. Chem. Soc.* **1984**, *106*, 2613.

Table 1. ^{1}H NMR Data for Ru(II)−Au(I) and Precursor Ruthenium Complexes in CD_3CN

	chemical shift (ppm)									
compound	H-2	H-9	H-4	H-7	H-5	H-6	H-3	H-8	H−C(≡C)	H-PPh_3
1	7.950	8.035	8.488	8.562	8.115	8.191		7.689		7.51−7.66
5	8.097	8.084	8.719	8.622	8.197	8.276		7.749	3.778	
2	7.997	8.076	9.038	8.487		8.227	7.671	7.763		7.50−7.62
6	8.098	8.131	8.872	8.564		8.481	7.739	7.806	4.126	
3	7.860	8.001	8.497	8.962	8.276			7.680		7.50−7.61
7	8.104	8.121	8.646	8.865	8.418			7.808	3.803 (3-H)	4.163 (6-H)

	H-2,9	H-4,7	H-5,6	H−C(≡C)	H-PPh_3
4	7.892	8.444	8.069		7.52−7.66
8	8.088	8.712	8.224	3.794	

(M^{2+}, 100%). FT-IR (KBr, cm^{-1}) ν(C≡C): 2105. UV/vis (CH_3CN): λ_{abs} nm ($\varepsilon \times 10^{-4}$) 452 (1.6), 428 (1.5), 340 (4.6), 315 (5.7), 288 (8.7). ^{1}H NMR (CD_3CN, 600 MHz, ppm): δ = 8.962 (dd, J = 8.3 Hz, 1H, phen-H7), 8.506 (m, 2H, bpy-H6), 8.497 (d, J = 1.6 Hz, 1H, phen-H4), 8.470 (m, 2H, bpy-H6′), 8.276 (s, 1H, phen-H6), 8.060 (m, 2H, bpy-H5), 8.001 (d, J = 4.2 Hz, 1H, phen-H9), 7.995 (m, 2H, bpy-H5′), 7.860 (d, J = 1.6 Hz, 1H, phen-H2), 7.816 (m, 1H, bpy-H3α), 7.770 (m, 1H, bpy-H3β), 7.680 (dd, J = 8.3 and 4.2 Hz, 1H, phen-H8), 7.677 (m, 1H, bpy-H3′α), 7.510 (m, 1H, bpy-H3′β), 7.409 (m, 2H, bpy-H4), 7.249 (m, 2H, bpy-H4′), 7.61−7.50 (m, 30H, phenyl-H).

Synthesis of [Ru(bpy)$_2${3,8-bis{(PPh_3)−Au−C≡C}-phen}]-(PF_6)$_2$ (4). Ruthenium complex **8** (93 mg, 0.10 mmol) and diisopropylamine (1.3 mL) were dissolved in a mixture solution of CH_3OH/CH_2Cl_2 (7:3) (30 mL) under N_2. The solution was added the CH_3OH/CH_2Cl_2 (7:3) solution (50 mL) of Au(PPh_3)Cl (99 mg, 0.20 mmol), and the mixture was stirred at 30 °C under N_2. After 3 days, an orange-red precipitate appeared in the solution. The precipitate was collected by filtration under low-pressure and washed with small amount of EtOH. The residue was redissolved in CH_2Cl_2 (60 mL) to remove insoluble impurities. The solvent was removed from the filtrate and a resulting orange-red powder was dried at 30 °C under vacuum for 5 h (95 mg, 51%). Anal. Calcd for $C_{72}H_{52}N_6P_4F_{12}Au_2Ru_1$: C, 46.46; H, 3.06; N, 4.69. Found C, 46.35; H, 2.94; N, 4.57%. Positive ESI-MS: ion at m/z 779.3 (M^{2+}, 100%). FT-IR (KBr, cm^{-1}) ν(C≡C): 2108. UV/vis (CH_3CN): λ_{abs} nm ($\varepsilon \times 10^{-4}$) 452 (1.5), 428 (1.4), 368 (5.1), 357 (5.4), 287 (10.1). ^{1}H NMR (CD_3CN, 600 MHz, ppm): δ = 8.513 (m, 2H, bpy-H6), 8.477 (m, 2H, bpy-H6′), 8.444 (d, J = 1.6 Hz, 2H, phen-H4 and phen-H7), 8.075 (m, 2H, bpy-H5), 8.069 (s, 2H, phen-H5 and phen-H6), 7.995 (m, 2H, bpy-H5′), 7.892 (d, J = 1.6 Hz, 2H, phen-H2 and phen-H9), 7.798 (m, 2H, bpy-H3), 7.645 (m, 2H, bpy-H3′), 7.434 (m, 2H, bpy-H4), 7.249 (m, 2H, bpy-H4′), 7.66−7.52 (m, 30H, phenyl-H).

Results and Discussion

Synthesis and Characterization. Dyads **1** and **2** were respectively synthesized by reacting the precursor ruthenium(II) polypyridyl complexes, **5** and **6** including a 3-ethynylphenanthroline and 5-ethynylphenanthroline, and Au(PPh_3)Cl. While the triads **3** and **4** were prepared by reacting the precursor complexes, **7** and **8** including a 3,6-diethynylphenanthroline and 3,8-diethynylphenanthroline, and two equivalent amounts of Au(PPh_3)Cl. (Chart 1). These Ru(II)−Au(I) compounds were characterized by ^{1}H NMR, IR, ESI-MS spectroscopy, and elemental analysis. Four compounds gave satisfying ESI-MS spectra and showed elemental analysis results in accordance with the assigned structures. IR spectral data of all Ru(II)−Au(I) compounds indicate that the metal−carbon bond between Au(I) ion and each ethynylphenanthroline is the η^1 coordination of σ-bonding. The characteristic ν(C≡C) bands were observed near 2100 cm^{-1}, and the ν(CC−H) bands at around 3270 cm^{-1} in the starting materials of ruthenium(II) complexes disappeared in Ru(II)−Au(I) compounds. The formation of the Au−C≡C bond is further supported by the ^{1}H NMR measurements. No assignable signal for the ethynyl proton was detected, and all observed signals in these compounds corresponded to the protons of their ethynyl-substituted phenanthrolines, bipyridine, and triphenylphosphine in accurate proportions. Upfield shifts were observed in all compounds for the protons of their phenanthroline ligands compared with precursor ruthenium(II) complexes, except for the signals assignable to the H-4 proton of **2** and H-7 of **3** (Table 1). These shifts could be triggered by the coordination of the gold(I) triphenylphosphine unit because of the π back-donation from the Au(I) center to each ethynyl-substituted phenanthroline. Additionally, the downfield shifts of the signals assignable to the H-4 proton of **2** and H-7 of **3** are due to high through-space deshielding by the gold(I) ethynyl substitution of the 5- and 6-positions, as indicated in our recent work.[20]

Absorption Spectroscopy. Figure 1 displays the absorption spectra of Ru(II)−Au(I) dyads and triads in CH_3CN at room temperature. The absorption bands in the 400−500 nm region of the Ru(II)−Au(I) compounds were assigned to typical MLCT transitions observed for ruthenium(II) polypyridyl complexes with bipyridine and/or phenanthroline derivatives. The absorption bands in the 300−400 nm region were primarily assigned to gold(I) perturbed $\pi-\pi^*$(C≡Cphen) transitions. The spectrum of triad **3** shows the lowest energy $\pi-\pi^*$(C≡Cphen) transition band near 340 nm. A similar absorption band for dyad **1** or **2** is detected in the same wavelength region, although the molar extinction coefficient for the lowest $\pi-\pi^*$ absorption of **3** is almost equivalent to the total of those of dyads **1** and **2** (Figure 1). As we have previously indicated, the lowest energy $\pi-\pi^*$ absorption near 360 nm for **4** shifted to a longer-wavelength area than that near 340 nm for **1**, which is likely due to greater electron delocalization by the two ethynyl substitutions on the phenanthroline skeleton.[14] Such a distinct red shift of the lowest $\pi-\pi^*$ absorption of **3** relative to that of **1** or **2** is not observed. The energy order of the lowest $\pi-\pi^*$(C≡Cphen)

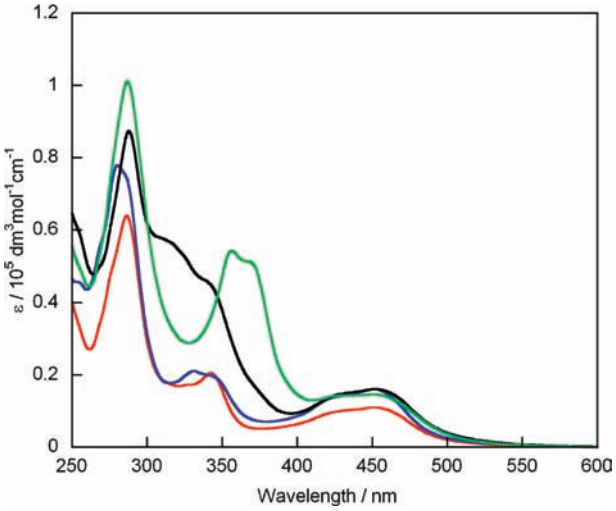

Figure 1. UV−vis absorption spectra of **1** (red), **2** (blue), **3** (black), and **4** (green) in CH_3CN at room temperature.

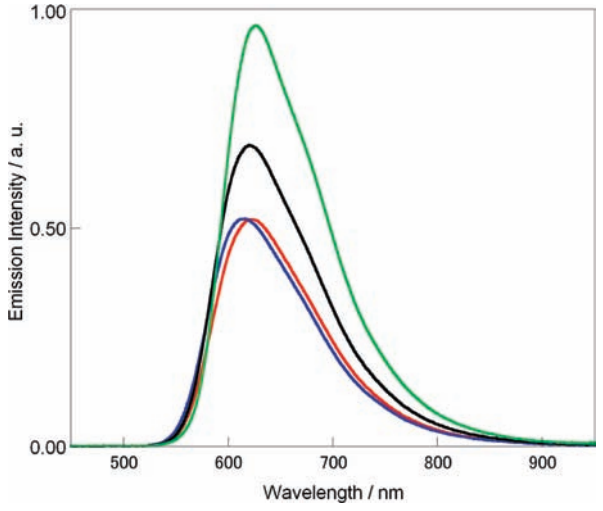

Figure 2. Emission spectra of **1** (red), **2** (blue), **3** (black), and **4** (green) in deoxygenated CH_3CN at room temperature.

transition band for Ru(II)−Au(I) compounds is represented as **2** ≈ **1** ≈ **3** > **4**, and this order is consistent with the energy order of the emission band in Ru(II)−Au(I) compounds, as indicated below.

Emission Spectroscopy. The Ru(II)−Au(I) compounds show visible broad emission bands centered around 620 nm (Figure 2) in deoxygenated acetonitrile at room temperature upon the excitation at 425 nm (**1**: 622 nm, **2**: 617 nm, **3**: 620 nm, **4**: 627 nm), respectively. These emissions were assigned to a typical triplet MLCT-based luminescence, which is well-known in the emissions for ruthenium(II) polypyridyl complexes with bipyridine and/or phenanthroline derivatives. Phosphorescence with vibronic progressions originating from the gold(I)-ethynylphenanthroline unit, the emissions of which were noted in our previous report regarding gold(I) complexes,[20,21] was not exhibited. Additionally, the excitation spectra of these compounds in the region between 300 and 500 nm were approximately compatible with the absorption spectra of these compounds in the same region. The hybrid architecture in Ru(II)−Au(I) compounds constructed with Ru(II)-polypyridyl and Au(I)-ethynyl units harvests near UV light and then converts the blue-green gold(I) perturbed $\pi-\pi^*$ phosphorescence into an orange MLCT-based emission. This energy transfer system from the Au(I)-ethynyl unit to the Ru(II)-polypyridyl unit operates effectively, although four ethynylphenanthroline ligands of the present triads and dyads have different ethynyl-substituted numbers or sites on the phenanthroline skeleton.

The emission data for all the ruthenium complexes (structure shown in Chart 1) and several mononuclear ruthenium complexes, $[Ru(bpy)_3](PF_6)_2$, $[Ru(bpy)_2L1](PF_6)_2$ (L1 = 3-*p*-tolylethynyl-phenanthroline), and $[Ru(bpy)_2L2](PF_6)_2$ (L2 = 3,8-bis-*p*-tolylethynyl-phenanthroline), are collected in Table 2. The quantum yields of the emissions, ϕ_{em}, and the emission decay, τ, were measured at room temperature in deoxygenated acetonitrile, and the radiative rate, k_r, and nonradiative rate, k_{nr}, were calculated with a standard formula.[24−26] The k_r values of all compounds fall within a narrow range due to their similar complex components, $[Ru(bpy)_2(N-N)](PF_6)_2$ (N−N = many types of these substituted phenanthroline).

The 0−0 band energy of the ^{3}MLCT transition, $E(0-0)$, is listed in Table 2. Emission spectral fitting parameters of all ruthenium complexes were calculated with the method of Franck−Condon analysis developed by Meyer's group.[24,25] Spectral fitting parameters at room temperature are listed in Supporting Information, Table S1 and typical calculated spectral fits of **3** at room temperature and 77 K are shown in Supporting Information, Figure S1, and details of the calculation are mentioned in the Supporting Information. The available parameters for $[Ru(bpy)_3](PF_6)_2$ are almost consistent with the data obtained previously by Meyer et al,[24] and the parameters ν_1 (1370−1400 cm^{-1}) and S_1 (0.75−1.05) fall within a narrow range for all the present compounds. Then, $E(0-0)$ are used to discuss the correlation between the electrochemical data and the 0−0 band energy of the ^{3}MLCT transition.

The S_1 values for the Ru(II)−Au(I) compounds (see Table 2) except for the S_1 (1.03) of **2** are clearly smaller than that (1.05) of $[Ru(bpy)_3](PF_6)_2$. In previous reports of Schoonover et al.,[27] the S_1 values of ruthenium and osmium complexes with phenanthroline derivatives are smaller than those of similar complexes with bipyridine derivatives at the same energy gap, and they explain that the difference between S_1 values is due to the greater rigidity of the phenanthroline skeleton compared to that of the bipyridine skeleton. Therefore, S_1 values smaller than 1.00 in the present ruthenium complexes except for **2** in Table 2 would demonstrate that the emission occurs from $^3[Ru^{III}(bpy)_2(N-N)^{\bullet-}]^*$. Similar interpretations are discussed in the electrochemical and the TA difference spectral data.

Correlation between Electrochemical and Photophysical Data. The electrochemical properties of the ruthenium(II) compounds were investigated by a cyclic voltammetry

(26) (a) Rillema, D. P.; Taghdiri, D. G.; Jones, D. S.; Keller, C. D.; Worl, L. A.; Meyer, T. J.; Levy, H. A. *Inorg. Chem.* **1987**, *26*, 578. (b) Ross, H. B.; Boldaji, M.; Rillema, D. P.; Blanton, C. B.; White, R. P. *Inorg. Chem.* **1989**, *28*, 1013.

(27) Schoonover, J. R.; Omberg, K. M.; Moss, J. A.; Bernhard, S.; Malueg, V. J.; Woodruff, W. H.; Meyer, T. J. *Inorg. Chem.* **1998**, *37*, 2585.

Table 2. Emission Data of Ru(II)−Au(I) and Mononuclear Ruthenium Complexes

compound	E(max)[a]/ eV	$E(0-0)$[b]/ eV	S_1[b]	ϕ_{em}[c]	τ[d]/ μs	k_r[e]/ 10^3 s^{-1}	k_{nr}[f]/ 10^4 s^{-1}
1	1.97	2.06	0.91	0.066	1.20	55	78
2	1.99	2.04	1.03	0.064	0.97	66	97
3	1.98	2.05	0.97	0.086	1.62	53	56
4	1.96	2.05	0.87	0.120	2.68	45	33
5	1.94	1.98	0.85	0.109	1.83	60	49
6	1.99	2.05	0.96	0.062	1.09	57	86
7	1.90	1.93	0.85	0.105	2.00	53	45
8	1.85	1.89	0.75	0.087	1.50	58	61
$Ru(bpy)_2L1$	1.95	1.98	0.87	0.140	2.35	60	37
$Ru(bpy)_2L2$	1.86	1.90	0.79	0.146	2.26	65	38
$Ru(bpy)_3$	1.99	2.04	1.05	0.062	0.96	65	98

[a] The E(max) is the energy of highest emission intensity on respective spectra. [b] The $E(0-0)$ and S_1 were calculated by Franck−Condon analysis (See Supporting Information). [c] The quantum yield of emission (ϕ_{em}) were determined by comparison with the value for $[Ru(bpy)_3](PF_6)_2$ (ϕ_{em} = 0.062). [d] The emission decays were calculated as single exponential. [e] $k_r = \phi_{em}/\tau$. [f] $k_{nr} = 1/\tau - k_r$.

Table 3. Electrochemical Data of Ru(II)−Au(I) and Mononuclear Ruthenium Complexes[a]

compound	$E_{1/2}$(ox) (V)	$E_{1/2}$(red) (V)	$\Delta E_{1/2}$ (V)
1	1.28	−1.32	2.60
2	1.28	−1.35	2.63
3	1.32	−1.25	2.57
4	1.35	−1.21	2.56
5	1.29	−1.18	2.47
6	1.28	−1.26	2.54
7	1.32	−1.08	2.40
8	1.32	−1.06	2.38
$Ru(bpy)_2L1$	1.27	−1.20	2.47
$Ru(bpy)_2L2$	1.30	−1.07	2.37
$Ru(bpy)_3$	1.26	−1.36	2.62

[a] Cyclic Voltammograms for all compounds were measured in 1.0 mM acetonitrile solutions containing 0.1 M Bu_4NPF_6, using a $Ag/AgNO_3/CH_3CN$ reference electrode (+0.37 V vs SCE; calibrated with $Fc^{0/+}$) and Pt working electrode.

technique in acetonitrile. Their electrochemical data are collected in Table 3, and a typical cyclic voltammogram including first oxidation and reduction waves of **3** is shown in the Supporting Information, Figure S2. Each complex exhibited reversible oxidation waves ($E_{1/2}$(ox)) and reversible first reduction waves ($E_{1/2}$(red)) in the potential range +1.50 V to −1.50 V versus SCE. The $E_{1/2}$(red) for all compounds occurs within a wide potential range between −1.06 and −1.36 V, while the $E_{1/2}$(ox) is observed at around +1.3 V (Table 3). The $E_{1/2}$(ox) for all compounds is typical for the $Ru^{3+/2+}$ couple of ruthenium(II) polypyridyl complexes with bipyridine and/or phenanthroline derivatives, while the $E_{1/2}$(red) is assigned to the first reduction process of the substituted phenanthroline ligand or one of the bipyridine ligands in each complex. The $E_{1/2}$(red) values of these ruthenium(II) compounds with substituted phenanthroline ligands were less negative than that of $Ru(bpy)_3(PF_6)_2$ (−1.36 V), although that of **2** (−1.35 V) was almost the same, which means that the substituted phenanthrolines have a better electron-accepting capability in comparison with bipyridine, except for 5-ethynylphenanthroline in **2**. Furthermore, the reduction potentials of all the Ru(II)−Au(I) compounds were more negative relative to those of the respective precursor ruthenium(II) complexes. This result supports the idea that these ethynyl-substituted phenanthrolines receive a π back-donation from the Au(I) center along with the coordination of the gold(I) triphenylphosphine unit in Ru(II)−Au(I) compounds, and this

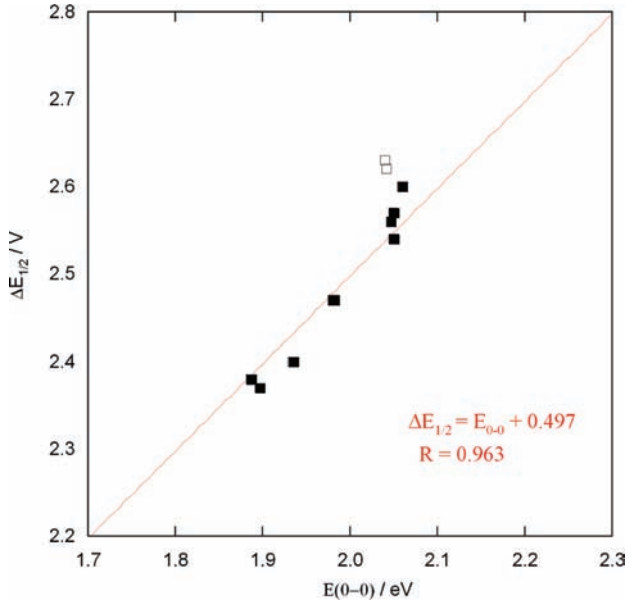

Figure 3. Plot of $E(0-0)$ versus $\Delta E_{1/2}$ for Ru(II)−Au(I) and mononuclear ruthenium complexes in CH_3CN at room temperature. Complexes are designated as follows: **2** and $Ru(bpy)_3$ (□); other compounds (■).

interpretation is consistent with the explanation of the upfield shifts discussed in the NMR experiment.

An interesting finding is that there is a good linear correlation, as shown in Figure 3, between the 0−0 band energy of the ^{3}MLCT transition, $E(0-0)$, and the potential difference between the oxidation and the first reduction potential, $\Delta E_{1/2}$. The $E(0-0)$ values for these complexes increase with increases in $\Delta E_{1/2}$; the value is more strongly influenced by the first reduction potential of the diimine ligands than by the oxidation of the $Ru^{3+/2+}$ couple, as mentioned above. A linear correlation between electrochemical and emission data has been found for most ruthenium(II) polypyridyl complexes by some research groups[24−29] and does exist when the molecular orbitals involved in the electrochemical process and those involved in the ^{3}MLCT transition of emissions are the same.[29] Therefore, the correlation indicates that

(28) Vlcek, A. A.; Dodsworth, E. S.; Pietro, W. J.; Lever, A. B. P. *Inorg. Chem.* **1995**, *34*, 1906.
(29) (a) Boisdenghien, A.; Moucheron, C.; Mesmaeker, A. K.-D. *Inorg. Chem.* **2005**, *44*, 7678. (b) Leveque, J.; Elias, B.; Moucheron, C.; Mesmaeker, A. K.-D. *Inorg. Chem.* **2005**, *44*, 393.

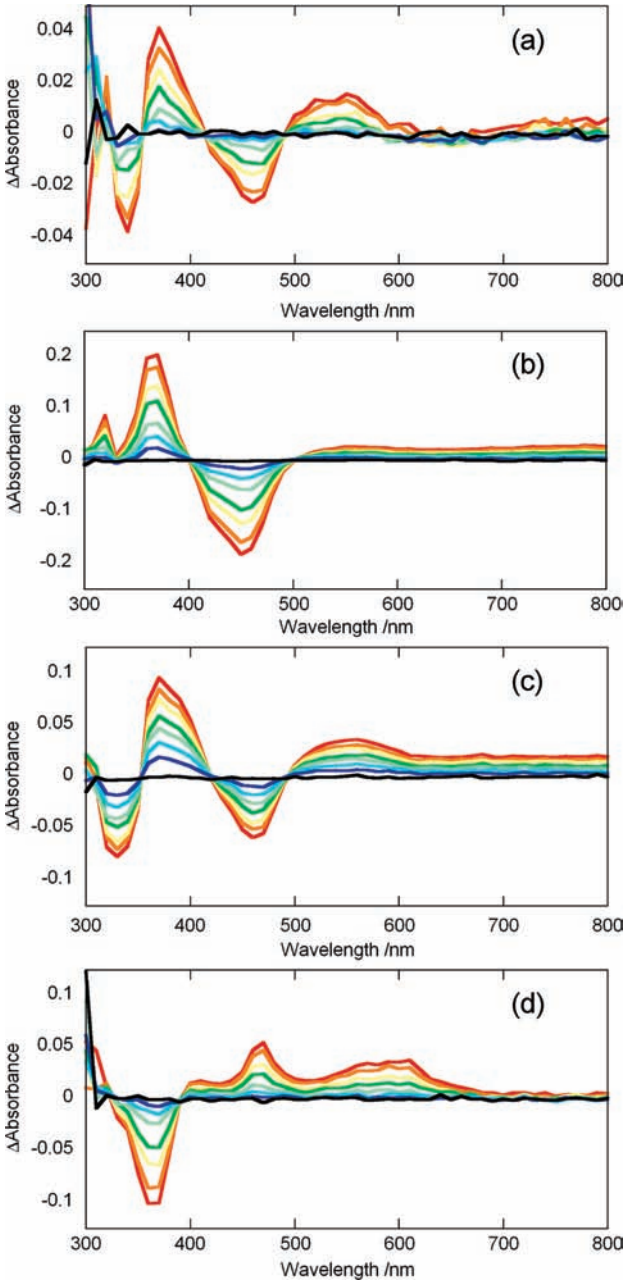

Figure 4. Transient absorption difference spectra of **1** (a), **2** (b), **3** (c), and **4** (d) in deoxygenated CH_3CN at room temperature.

the ^{3}MLCT emissions are based on the charge transfer from the ruthenium center to the substituted phenanthroline ligand in almost all of these complexes. The spot of **2** in Figure 3, however, appears to deflect from the correlation line the same as that of $Ru(bpy)_3(PF_6)_2$, although the departure is not large. This deflection of **2** and $Ru(bpy)_3(PF_6)_2$ must show that the ^{3}MLCT emissions in these complexes are based on the charge transfer from the ruthenium center to one of the bipyridine ligands. The validity of this explanation is supported by the observation of the TA difference spectra, as mentioned below.

TA Difference Spectroscopy. Figure 4 displays the TA difference spectra of Ru(II)−Au(I) dyads and triads at room temperature in deoxygenated CH_3CN. The TA spectrum of **1** was distinctly different from that of $[Ru(bpy)_3](PF_6)_2$ reported in previous works,[30,31] while the TA spectrum of **2** was very similar to that of $[Ru(bpy)_3](PF_6)_2$. There appear to be three main differences between the spectra of **1** and **2**.

(i) The strong bleaching of the gold(I) perturbed $\pi-\pi^*$(C≡Cphen) absorption band near 340 nm in **1** (Figure 4(a))

(ii) The strong absorption near 370 nm assignable to the $\pi-\pi^*$ (bpy anion radical) transition under the triplet excited state of **2** (Figure 4(b)); this absorption is also the characteristic band in the TA spectrum of $[Ru(bpy)_3](PF_6)_2$.

(iii) The definite absorption over 500 nm, which is probably assignable to the $\pi-\pi^*$ (C≡Cphen anion radical) transition, under the triplet excited state of **1** (Figure 4(a))

Corresponding distinctions were also confirmed between the spectra of **2** and **3** (Figure 4(b, c)), and the TA spectrum of **3** was similar to that of **1** (Figure 4(a, c)). The TA spectrum of **4** showed the bleaching of the $\pi-\pi^*$(C≡CphenC≡C) absorption band near 360 nm and a marked absorption band over 400 nm, which is probably assignable to a $\pi-\pi^*$(C≡CphenC≡C anion radical) absorption. The lowest energy $\pi-\pi^*$-(C≡CphenC≡C anion radical) absorption band near 600 nm of **4** was shifted from the $\pi-\pi^*$ (C≡Cphen anion radical) absorption near 550 nm of **1**, and the red shift is likely due to greater electron delocalization by the two ethynyl substitutions on the phenanthroline skeleton. Such a distinct red shift of the $\pi-\pi^*$ absorption between **1** and **3** was not observed. Additionally, the lifetimes calculated from these TA difference spectra of four Ru(II)−Au(I) compounds are respectively in agreement with their emission lifetimes τ_{em} measured by a time-resolved emission experiment of these compounds, the results of which are shown in Table 2.

The noticeable bleaching of the Ru(II)−Au(I) compounds except for **2** in the 300−400 nm region supports the idea that Ru(II)−Au(I) compounds **1**, **3**, and **4** receive the supposed charge injection from a ruthenium center to an extended π-conjugated ethynyl-substituted phenanthroline which contains one or two gold(I) organometallic unit(s) under the MLCT excited state. The similarity of the TA spectra between **2** and $[Ru(bpy)_3](PF_6)_2$ should be interpreted as an electron from the ruthenium center being transferred not to the 5-ethynylphenanthroline but to one of the bipyridyl ligands in **2** under the MLCT excited state.

Conclusions

The Ru(II)−Au(I) dyad **2** and triad **3** have been prepared, and the photophysical properties of four Ru(II)−Au(I) supramolecular complexes including **1** and **4** have been characterized. These dyads and triads showed typical MLCT absorptions and a gold(I) perturbed $\pi-\pi^*$ absorption. These compounds also showed a broad phosphorescent band assignable to a triplet MLCT transition, which means that

(30) Kumar, C. V.; Barton, J. K.; Turro, N. J.; Gould, I. R. *Inorg. Chem.* **1987**, *26*, 1455.

(31) Ohno, T.; Yoshimura, A.; Prasad, D. R.; Hoffman, M. Z. *J. Phys. Chem.* **1991**, *95*, 4723.

the hybrid architecture in the Ru(II)−Au(I) supramolecular system constructed with Ru(II)-polypyridyl and Au(I)-ethynyl units is transferred from the energy of blue-green gold(I) perturbed $\pi-\pi^*$ luminescence to that of an orange MLCT-based emission. It is appropriate to highlight the difference in the electron transfer process in these Ru(II)−Au(I) compounds under the triplet MLCT state. Three compounds, **1**, **3**, and **4**, were found to receive a supposed charge injection from a ruthenium center to an extended π-conjugated ethynyl-substituted phenanthroline containing one or two gold(I) organometallics unit(s), while the dyad **2** undergoes the electron transfer process from the ruthenium center to one of the bipyridyl ligands under the MLCT excited state. This notion is supported by the difference of S_1 values among these compounds, the deflection of the spot of **2** from the linear correlation line in a plot of $E(0-0)$ versus $\Delta E_{1/2}$, and the similarity of the TA difference spectra between **2** and $[Ru(bpy)_3](PF_6)_2$. We are currently extending the synthetic work of novel Ru(II)−Au(I) compounds in which a gold(I) ion simply coordinates to two ethynylphenanthroline ligands without a phosphine ligand.

Acknowledgment. This work was supported in part by a Grant-in-Aid for Scientific Research (C) 20550062 from the Ministry of Education, Culture, Sports, Science, and Technology, Japan.

Supporting Information Available: Emission data and emission spectral fitting parameters at room temperature and at 77 K, emission spectra and calculated spectral fits of **3** at room temperature and at 77 K, and the cyclic voltammograms of **3** at room temperature. This material is available free of charge via the Internet at http://pubs.acs.org.